sustainability

Article

Spatiotemporal Surveillance of COVID-19 Based on Epidemiological Features: Evidence from Northeast Iran

Mohammad Tabasi [1], Ali Asghar Alesheikh [1], Elnaz Babaie [1] and Javad Hatamiafkoueieh [2,*]

[1] Department of GIS, Faculty of Geodesy and Geomatics Engineering, K. N. Toosi University of Technology, Tehran 19967-15433, Iran

[2] Department of Mechanics and Control Processes, Academy of Engineering, Peoples' Friendship University of Russia (RUDN University), Miklukho-Maklaya Str. 6, Moscow 117198, Russia

* Correspondence: khatamiafkuiekh-d@rudn.ru

Abstract: Spatiotemporal analysis of COVID-19 cases based on epidemiological characteristics leads to more refined findings about health inequalities and better allocation of medical resources in a spatially and timely fashion. While existing literature has explored the spatiotemporal clusters of COVID-19 worldwide, little attention has been paid to investigate the space-time clusters based on epidemiological features. This study aims to identify COVID-19 clusters by epidemiological factors in Golestan province, one of the highly affected areas in Iran. This cross-sectional study used GIS techniques, including local spatial autocorrelations, directional distribution statistics, and retrospective space-time Poisson scan statistics. The results demonstrated that Golestan has been facing an upward trend of epidemic waves, so the case fatality rate (CFR) of the province was roughly 2.5 times the CFR in Iran. Areas with a more proportion of young adults were more likely to generate space-time clusters. Most high-risk clusters have emerged since early June 2020. The infection first appeared in the west and southwest of the province and gradually spread to the center, east, and northeast regions. The results also indicated that the detected clusters based on epidemiological features varied across the province. This study provides an opportunity for health decision-makers to prioritize disease-prone areas and more vulnerable populations when allocating medical resources.

Keywords: health inequality; COVID-19; epidemiological features; spatiotemporal dynamics; GIS

check for updates

Citation: Tabasi, M.; Alesheikh, A.A.; Babaie, E.; Hatamiafkoueieh, J. Spatiotemporal Surveillance of COVID-19 Based on Epidemiological Features: Evidence from Northeast Iran. *Sustainability* **2022**, *14*, 12189. https://doi.org/10.3390/su141912189

Academic Editors: Jianquan Cheng, Jon Bannister and Daniel Diaz

Received: 30 June 2022
Accepted: 17 September 2022
Published: 26 September 2022

1. Introduction

Severe Acute Respiratory Syndrome Coronavirus 2 (SARS-CoV-2) first emerged in December 2019 in Wuhan, Hubei Province, China. Immediately after the start of the pandemic in China, Iran experienced an explosive surge in morbidity and mortality of the disease. In mid-February 2020, Iran was identified as the second center of COVID-19 dissemination worldwide after China [1].

Although quarantine, early testing, and exploring the transmission trajectories are urgently required to tackle the infection [2], rapid and perfect implementation of these strategies by developing countries such as Iran in the early stages of the pandemic seems complicated. A quick surveillance of disease dynamics provides meaningful findings for health agencies to explore disease-prone areas, apply efficient and accurate spatial interventions, and prioritize high-risk locations for resource allocation [3].

Geographical Information System (GIS) is a valuable tool in medical geography, which sheds light on the spatiotemporal behavior of diseases [4–7]. Investigating only one aspect of the spatial [8,9] and temporal [10,11] trend of COVID-19 cannot present the spatial and temporal variations of the infection simultaneously. However, space-time clustering analysis can identify both spatial and temporal clusters simultaneously, providing a more accurate assessment of the outbreak by time and space [3]. Therefore, exploring the spatiotemporal clusters of the COVID-19 outbreak, as unfolding in communities, is crucial for timely targeted interventions [12]. While the space-time analysis of the pandemic has been conducted in many countries, including the United States [13], China [14], Hong Kong [15], Brazil [16], Japan [17], Bangladesh [18], and Sweden [19], relatively little attention has been paid to elucidate the spatiotemporal clusters of COVID-19 in Iran, where it still faces new waves of the pandemic [20].

There is a vast body of studies indicating that severe outcomes of the virus are associated with the epidemiological characteristics of patients, including age, sex, and comorbidities (e.g., diabetes and hypertension) [21,22]. Studying the disease behavior based on epidemiological features can not only reveal health inequalities but also provide helpful information for health policymakers to identify at-risk populations. Little attention has been paid to exploring the spatiotemporal disparities of COVID-19 according to epidemiological characteristics. In this regard, studies [18,19,23] only focused on the spatiotemporal clustering of COVID-19 cases and deaths exclusively. For example, [14] explored the clusters of COVID-19 cases in China using the retrospective space-time scan statistic. Their results indicated that high-risk spatiotemporal clusters were mainly distributed in densely populated provinces with developed transportation services. Another study [15] identified the clusters of COVID-19 cases in Hong Kong. According to their results, high and dense buildings, higher land use mix, and high access to transportation networks increase the risk of contracting the virus. Besides, studies on the space-time detection of COVID-19 clusters have recommended that future works should investigate the disease clusters by age, sex, and preexisting medical conditions [12,13,24]. Exploring the spatiotemporal disparity of the cases according to epidemiological factors in developing countries with limited medical resources at their disposal is empirically unknown, which will make a substantial contribution.

Studying space-time clusters of diseases on a more detailed spatial scale allows authorities to design more explicit prevention strategies. Due to the unavailability of data, most of the existing studies have detected spatial, temporal, and spatiotemporal clusters of COVID-19 on the administrative boundaries of countries [25], districts [18], and counties [13]. Therefore, identifying the disease clusters on a finer spatial scale is essential. Most of the related works have studied the clusters of COVID-19 up to six months after the onset of the epidemic [12,15,25]. It may impede a holistic view of the temporal evolution of the virus over a long period.

This study addresses the research gap by using spatial analysis and space-time scan statistics to visualize the temporal and spatial evolution of COVID-19 and to explore candidate clusters of the disease cases by age, sex, urban/rural housing, comorbidities, and patient outcome in northeast Iran, Golestan province, over a long-term period of 13 months at the village level, which is the most minor administrative division in Iran. The study's findings generate critical insights for health authorities on how epidemiological features may affect residents' health in disease-prone areas and lead to the development of targeted interventions in response to COVID-19 transmission.

2. Materials and Methods

2.1. Study Area

Golestan province geographically lies between 36°30′ N–38°08′ N latitude and 53°57′ E–56°22′ E longitude, as shown in Figure 1. This province has a population of 1.869 million residents in its territory of 20,367 km^2. The province has 14 counties divided into 60 rural districts, which are further split into 32 cities and 992 villages, which is the study unit of the analysis [26].

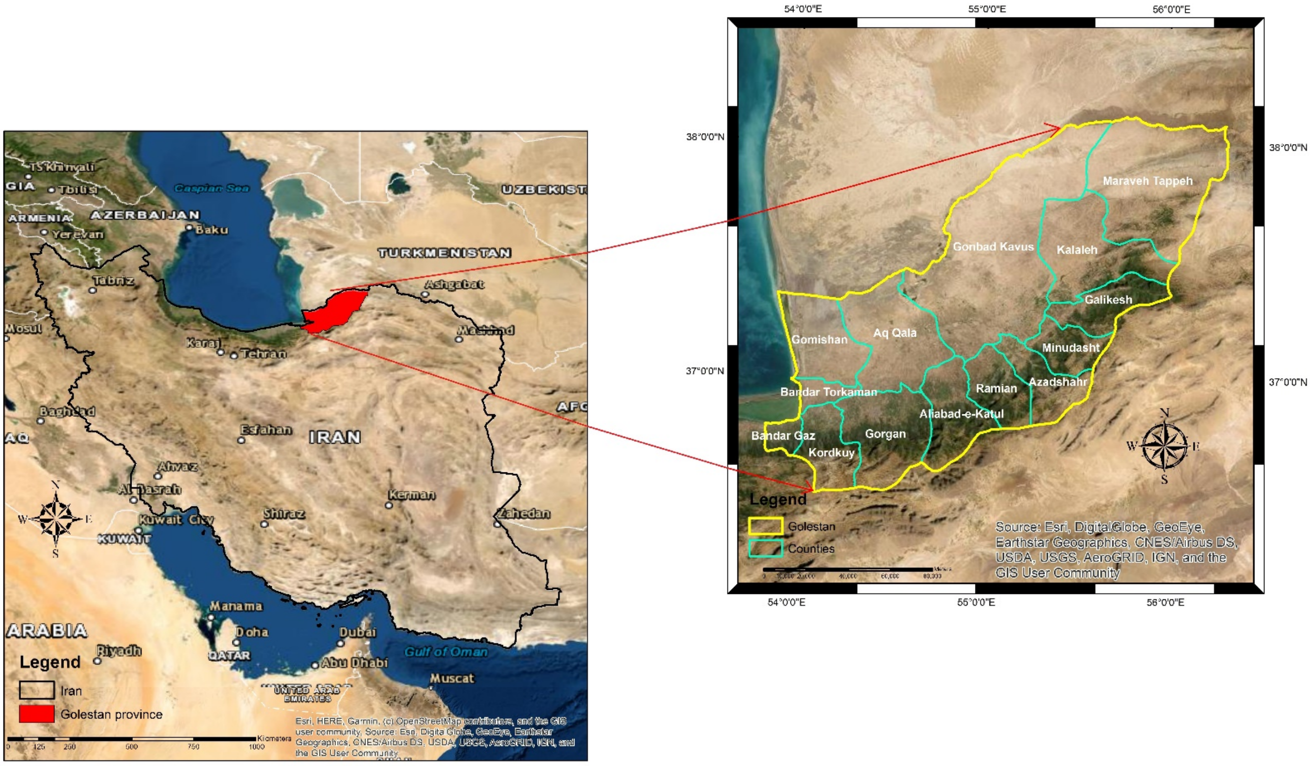

Figure 1. Location of Golestan province and its counties.

2.2. Data Acquisition

COVID-19 data on 21,987 daily confirmed cases from the onset of the infection on 1 February 2020 to 28 February 2021 in the study area were gathered from the Center for Disease Control and Prevention (CDC) of Golestan province [27]. This data includes age (i.e., consisting of 8 age groups of 0–9 to 70 and above), sex (male/female), urban/rural housing (rural/urban), diagnosis date, location, patient outcome (recovered at home, hospital discharge, and death), and preexisting medical conditions (cancer, cardiovascular disease, diabetes, hypertension, immunodeficiency, kidney disease, liver disease, lung disease, and neurological disorders). This data consists of patients hospitalized due to the virus and people who referred to COVID-19 test centers, and the result of their COVID-19 test was positive. The population of the villages' and cities' residents was collected from the Statistical Center of Iran in 2016 (the last year of the census in Iran) [28]. Spatial data (shapefiles) about villages' and cities' locations (point) was obtained from the Deputy of Statistics and Information of Golestan Province [26]. To explore high-risk areas of transmission, we calculated the incidence rate for each village/city. The incidence rate is the number of new cases over a specified period divided by the population at risk over that period multiplied by 100,000 [29]. We assumed that residents of villages/cities are the exposed populations (population at risk) because COVID-19 threatens all age groups and all genders during the pandemic. We also assume that the population of each village/city is constant during the study period. We aggregated the COVID-19 dataset at the village/city level (point layers). In this regard, we geo-coded all the patients based on their locations (cities or villages) and assigned them latitude and longitude coordinates using ArcGIS 10.2 (ESRI, Redlands, CA, USA).

2.3. Methodology

This study was conducted in three steps. First, we demonstrated the temporal evolution of COVID-19 cases using statistical graphs. Second, hot spot analysis was used to explore high and low-risk areas of the disease across the Golestan province. We also applied directional distribution analysis to identify the distributional trend of COVID-19 throughout the province. Finally, a retrospective space-time Poisson scan statistic was used to explore spatiotemporal clusters of COVID-19 cases based on epidemiological features.

2.3.1. Hot Spot Analysis

We used the Getis Ord Gi* statistic [30] to locally demonstrate hot spots and cold spots (high and low-risk areas). This statistic is a proper choice chosen to identify the structure of COVID-19 clusters locally [30], which is calculated based on Equations (1)–(3):

$$\mathrm{Gi}^* = \frac{\sum_{j=1}^{n} Wi,j\,Xj - X\sum_{j=1}^{n} W\,i,j}{S\sqrt{\frac{\left[n\sum_{j=1}^{n} W\,i,j^2 - \left(\sum_{j=1}^{n} W\,i,j\right)^2\right]}{n-1}}}, \tag{1}$$

$$\mathrm{X} = \frac{\sum_{j=1}^{n} Xj}{n}, \tag{2}$$

$$\mathrm{S} = \sqrt{\frac{\sum_{j=1}^{n} Xj^2}{n} - (\mathrm{X})^2}\,, \tag{3}$$

where x_j reflects the incidence rate of feature j (village/city), n denotes the total number of features, and $w_{i,j}$ is the spatial weight between features i and j. We used the fixed distance band method as the conceptualization of spatial relationships among the features, which ensures each feature has at least one neighbor. We used the projected data to accurately measure distances based on Euclidean distances. This analysis returns three measures of z-score (Gi*), p-value, and confidence level bin (Gi_Bin) for each feature. A high positive z-score with a low p-value indicates a spatial clustering of high values. A low negative z-score with a low p-value indicates a spatial clustering of low values. A z-score close to zero indicates that there is no significant spatial clustering. The more intense clustering is directly related to the higher or lower z-scores. The Gi_Bin between −3 and +3 indicates statistical significance with a confidence level of 99%. The Gi_Bin between −2 and +2 indicates statistical significance with a confidence level of 95%. Gi_Bin between −1 and +1 indicates statistical significance with a confidence level of 90%. The Gi_Bin equal to zero reflects no apparent spatial clustering.

2.3.2. Directional Distribution Analysis

To explore the distributional trend of the COVID-19 outbreak across the Golestan province, we used the Directional distribution (Standard deviational ellipse) statistic [31]. Using the ellipse, it is possible to examine whether the spatial distribution of the disease is elongated and therefore has a specific orientation [31]. We analyzed the ellipses based on the weight (z-score) of features (villages/cities), which reflects the intensity of clustering. The size of ellipses was calculated based on one standard deviation that covers approximately 68% of all the features [31]. To accurately measure distances, we used a projected coordinate system for the input features.

2.3.3. Space-Time Analysis

For space-time analysis, COVID-19 cases were categorized by age, sex, urban/rural housing urban/rural housing, patient outcome, and comorbidities. The retrospective space-time scan statistic [32] was used to identify spatiotemporal clusters of COVID-19 cases based on epidemiological factors. This statistic has been widely used to detect clusters of infectious diseases [3,33]. The retrospective scan statistic identifies historical clusters that emerged at any time during the study period [34], while the prospective scan statistic scans the study area for active or emerging clusters that were still active by the end of the study period [35]. Since the study period completely covers four waves of the pandemic across the Golestan province (Figure 2), and no emerging clusters have been observed until the end of the examined period, we leveraged this statistic instead of the prospective space-time analysis [36]. In this regard, the retrospective analysis is more compatible with our data.

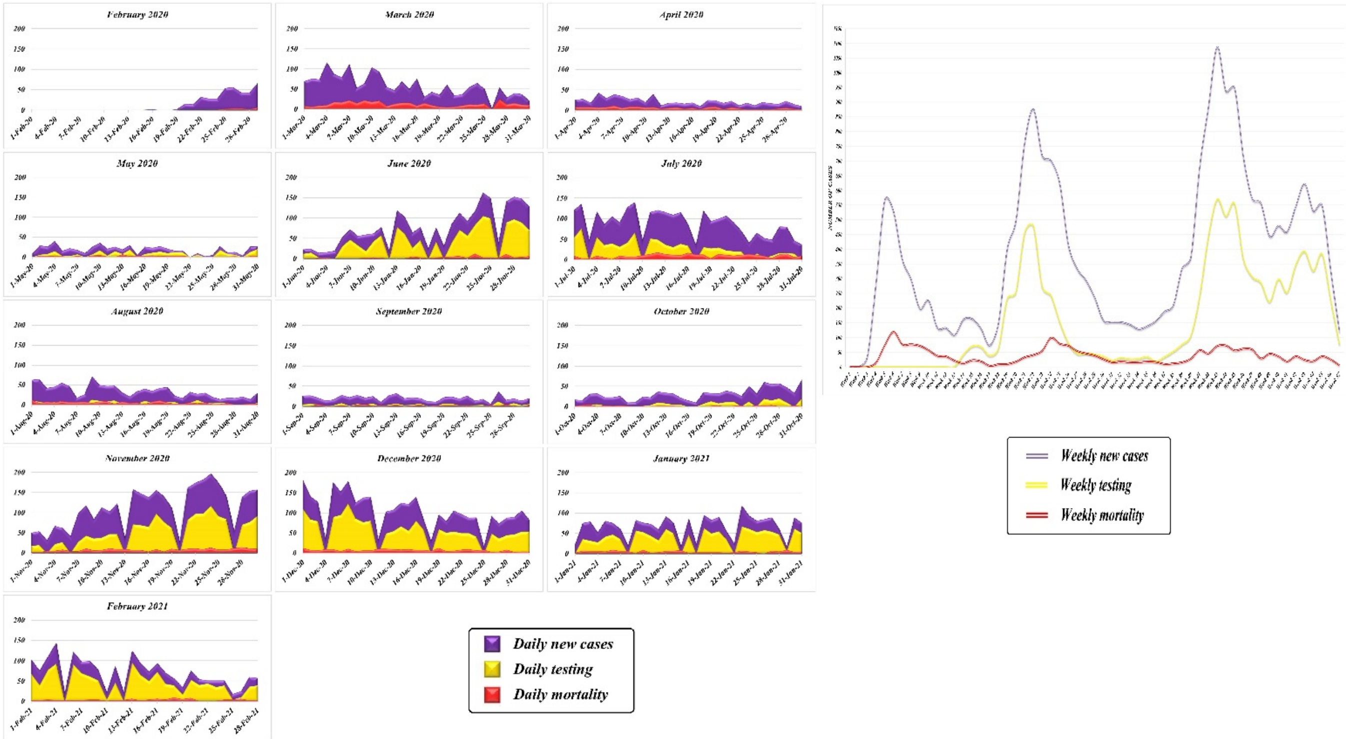

Figure 2. Temporal evolution (daily and weekly) of the COVID-19 transmission by total new cases, cases in test centers, and deaths in Golestan province between 1 February 2020 and 28 February 2021. The vertical axis represents the number of cases, and the horizontal axis corresponds to the study period.

The space-time scan statistic identifies significant clusters of elevated risk using cylinders (i.e., scanning windows) scanning the study area. The circular (or elliptic) base and height of each cylinder capture the spatial and temporal dimensions of the clusters, respectively [32]. As the scan progresses, each cylinder covers a different set of clusters that can be identified as candidate clusters. The center of each candidate cluster is co-located with the centroid of each village/city (point layer) in the study area. We identified space-time clusters using a discrete Poisson model, which has been used in previous studies [12,13]. Accordingly, we assumed that the COVID-19 cases follow a Poisson distribution. Under the null hypothesis (H_0), the expected number of cases (E[c]) in each area is proportional to the at-risk population in that area, as presented in Equation (4). A cluster is identified as a candidate cluster when the number of observed cases exceeds the expected number of cases in that cluster (alternative hypothesis, H_A).

$$\mathrm{E[c]} = p * \frac{C}{P} \tag{4}$$

where p is the population of each village/city; C reflects the total number of COVID-19 cases in the study area; P represents the total population of the study area. We assumed the population was static for each village/city across the study period. To detect clusters with an elevated risk, a likelihood ratio test for each cylinder was calculated, as defined in Equation (5).

$$\frac{L}{L_0} = \frac{\left(\frac{c}{E[c]}\right)^c \left(\frac{C-c}{C-E[c]}\right)^{C-c}}{\left(\frac{C}{E[C]}\right)^C}, \tag{5}$$

where L is the likelihood function for a cylinder; L_0 is the likelihood function for H_0; c is the number of cases in a cylinder; $E[c]$ is the expected number of cases in a cylinder; C reflects the total number of COVID-19 cases in the study area across the study period; $E[C]$ is the total number of expected cases in the study area across the study period. The risk for a cylinder increases when its likelihood ratio reaches greater than 1. A cylinder with the maximum likelihood ratio is identified as the most likely cluster. According to Equation (6), a relative risk (RR) was calculated for each cluster, which is defined as the estimated risk in a cluster divided by the risk outside of that cluster.

$$\mathrm{RR} = \frac{\frac{c}{E[c]}}{\frac{C-c}{C-E[c]}}, \tag{6}$$

where c is the number of cases in a cluster; $E[c]$ is the expected number of cases in a cluster; C is the total number of cases in the study area. For example, if a cluster has an RR of 3.5, the population within this cluster is 3.5 times more likely to be exposed to the disease than the population outside that cluster.

Similar to [12], candidate clusters should have at least five confirmed cases, and the minimum duration of clusters is set to 2 days. We considered the circular spatial window, which scans for areas with high rates. In the case of the actual operability of disease surveillance and to avoid extremely large clusters which might not be useful for health policymakers, the maximum spatial scanning window was set to 10% of the population at risk. The temporal scanning window was set to 50% of the entire study period. A total of 999 runs of Standard Monte Carlo simulations were used to assess the statistical significance of the candidate clusters with a p-value ≤ 0.05. To demonstrate significant space-time clusters across the Golestan province, we employed ArcGIS 10.2.

3. Results

3.1. Temporal Trend

From the first confirmed case to 28 February 2021, four epidemic peaks were observed over Golestan province, as shown in Figure 2. The pandemic required just one month to reach its first peak on 4 March 2020, with 116 daily new cases. The next two peaks emerged at approximately four-month intervals, whereas the fourth peak appeared two months after the tertiary peak. The highest peak in daily new cases (197) occurred on 24 November 2020 (Figure 2). Correlation analysis demonstrated a highly positive correlation of 0.88% (p-value ≤ 0.05) between the weekly new case and weekly testing. There is also a significant positive correlation between the weekly new case and weekly mortality (0.58%, p-value ≤ 0.05).

3.2. Spatial Analysis

The distributional trend of the high and low-risk villages/cities for the monthly incidence rate and its average across the Golestan province over the thirteen-month time frame have been illustrated in Figure 3. These maps indicate that the occurrence of COVID-19 varied geographically throughout the province during the investigation period. No village or city was immune. The hot spots were aggregated in the southwestern, eastern, and southeastern sectors of Golestan. By the end of February 2020, hot spots were mainly located in Gorgan, the capital city of Golestan province, and its bordering cities and villages. However, over the next two months, high-risk areas were elongated to the eastern parts of the province. From the beginning of May 2020 to the end of July 2020, the high-risk areas were moved to the central, eastern, and northeastern regions. From the beginning of August to the end of November, no significant high-risk clusters were seen in the southern and western parts. However, with the start of the third wave of the pandemic in late November (Figure 2), clusters of high-risk areas emerged in the western regions and reached the eastern regions by the end of February 2021. Generally, COVID-19 was progressing from the west and southwestern areas, having a higher incidence rate, towards the east and southeastern areas, containing a lower disease outbreak.

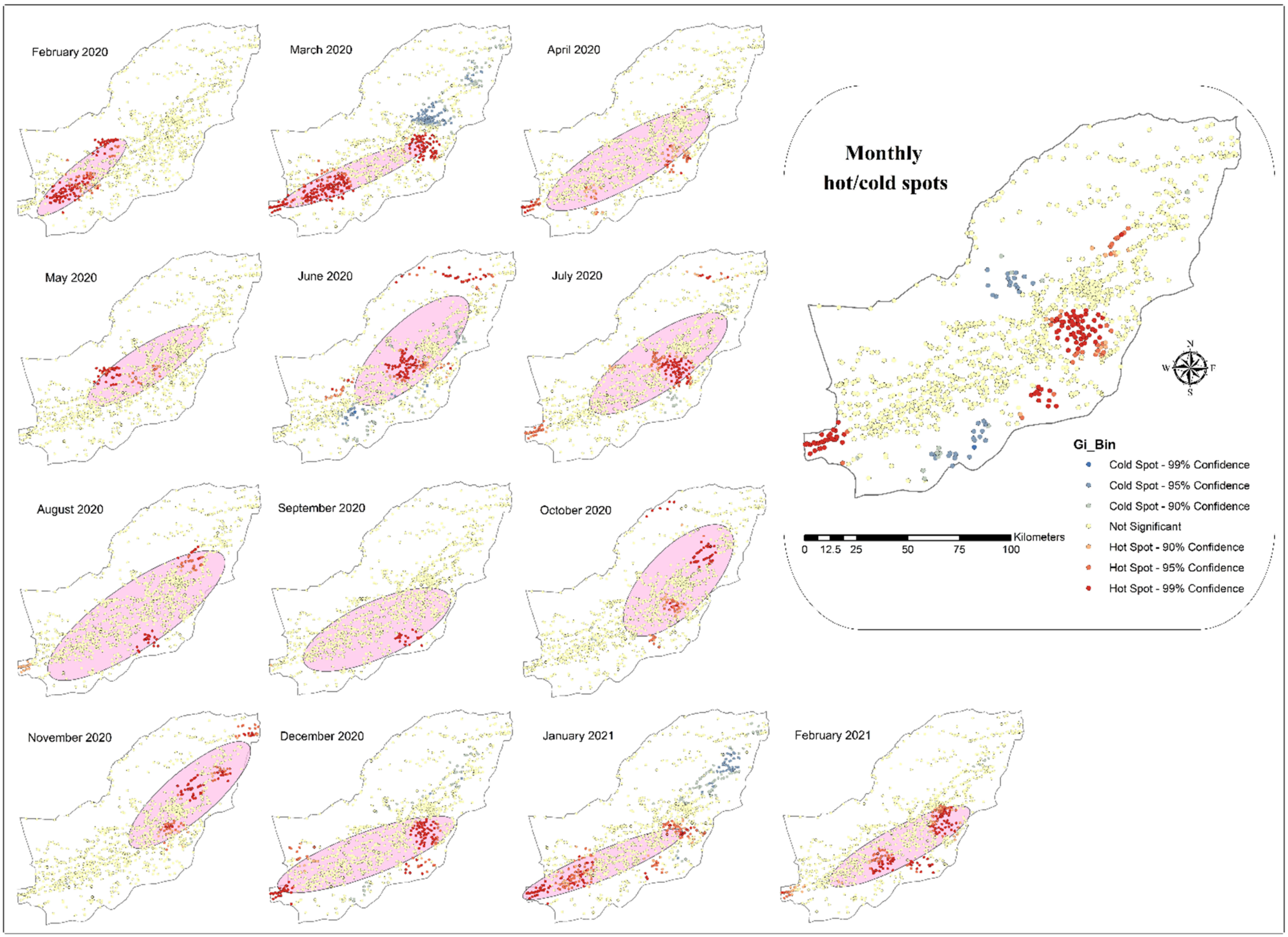

Figure 3. The spatial and directional distribution of hot/cold spots for the monthly incidence rate of COVID-19 across Golestan province from 1 February 2020 to 28 February 2021. Red and blue points correspond to high and low-risk villages/cities, respectively.

3.3. Spatiotemporal Analysis

A total of 12 statistically significant (p-value ≤ 0.05) space-time clusters were identified for all COVID-19 cases across the Golestan province during the study period. The most likely cluster spans a small area with six villages and one city (Gonbad-e Kavus city) in the east-central areas of the province (Figure 4 and Table S2, Supplementary Materials), which lasted from early June 2020 to late July 2020. This cluster belongs to the second pandemic wave in the study area (Figure 2). The 11 secondary clusters were detected in the north, west, central, and east of the province. Most of them (9 clusters) appeared in the third and fourth waves of the pandemic in the province, as summarized in Table S2.

As shown in Figure 5, spatiotemporal clusters by varying age groups did not follow the same distribution over the province. Only one significant cluster was observed for the age group of 0 to 9 years. Unlike other age groups, the most likely cluster related to the age group of 60–69 appeared in the third wave of the pandemic and was located in the northwest of Golestan. Except for the age group of 60–69, all the most likely clusters were predominantly in the east-central regions of the province. They followed the same temporal trend (the second wave of the pandemic) as the detected clusters for all confirmed cases, albeit with a slight difference (Figures 4 and 5 and Table S2).

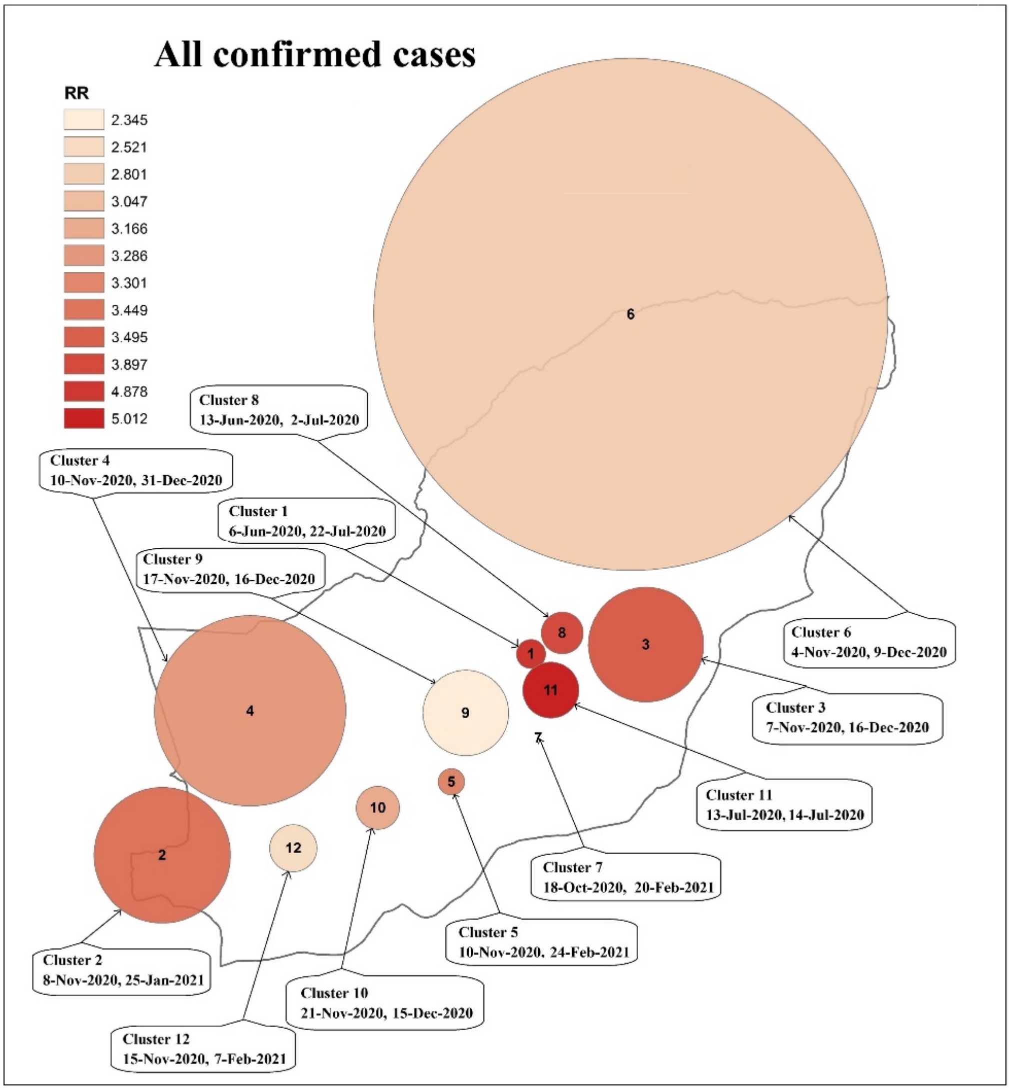

Figure 4. Spatiotemporal clusters of all COVID-19 cases along with their relative risk across the villages/cities of Golestan province between 1 February 2020 and 28 February 2021.

With regard to gender, the clusters observed for the female class have closely mirrored the clusters of all COVID-19 cases in size, location, and time (Figures 4 and 6 and Table S2). For example, the most likely clusters for the female class and the overall cases were approximately located in the same areas (the east-central sectors of the province). They also had the same period (Early June 2020 to late July 2020). Among all the significant clusters, the most likely cluster of the male class lasted the longest (194 days) (Table S2).

According to Figure 7 and Table S2, the most likely cluster of urban residents with a high relative risk (RR = 6.179) was located in the southwest of the province, which compromises only one city (Bandar-e Gaz). This cluster was related to the third and fourth waves of the pandemic. On the other hand, the primary cluster of rural areas covered 42 villages in the eastern-central regions of the province and appeared in the second wave of the pandemic.

The most likely clusters for all three classes of "Recovered at home", "Hospital discharge", and "Death" were located almost in the eastern-central regions of Golestan and emerged simultaneously in one month (June 2020), with the difference that the most likely cluster corresponding to the "Hospital discharge" lasted longer than the most likely clusters of "Death" and "Recovered at home" (196, 60, and 26 days, respectively) (Table S2 and Figure S3, Supplementary Materials). The significant clusters related to "Death" mainly occurred in the first wave of the pandemic, while the significant clusters of the “Recovered at home” were mainly observed in the third and fourth waves. On the other hand, the significant clusters of “Hospital discharge” usually appeared throughout the studied period (Table S2 and Figure 2).

The clusters of patients with comorbidities did not follow the same spatiotemporal distribution in Golestan over the investigation period, as shown in Figure S4 (Supplementary Materials) and Table S2. The significant clusters of “Diabetes” and “Cardiovascular disease” were mainly concentrated in the western, southwestern, and eastern-central areas of the province, while clusters corresponding to “Hypertension” were observed throughout the province. Two significant clusters were identified for “Liver disease” in the eastern-central regions. In addition, only one most likely cluster was detected for “Neurological disorders”, “kidney disease”, and “lung disease”, located in the northeast, southwest, and central areas, respectively. No significant clusters were observed for “Cancer” and “Immunodeficiency”. All the significant clusters of “Cardiovascular disease” were identified in the first and second waves of the pandemic, while the significant clusters of “Hypertension” emerged in the third and fourth waves (Table S2 and Figure 2).

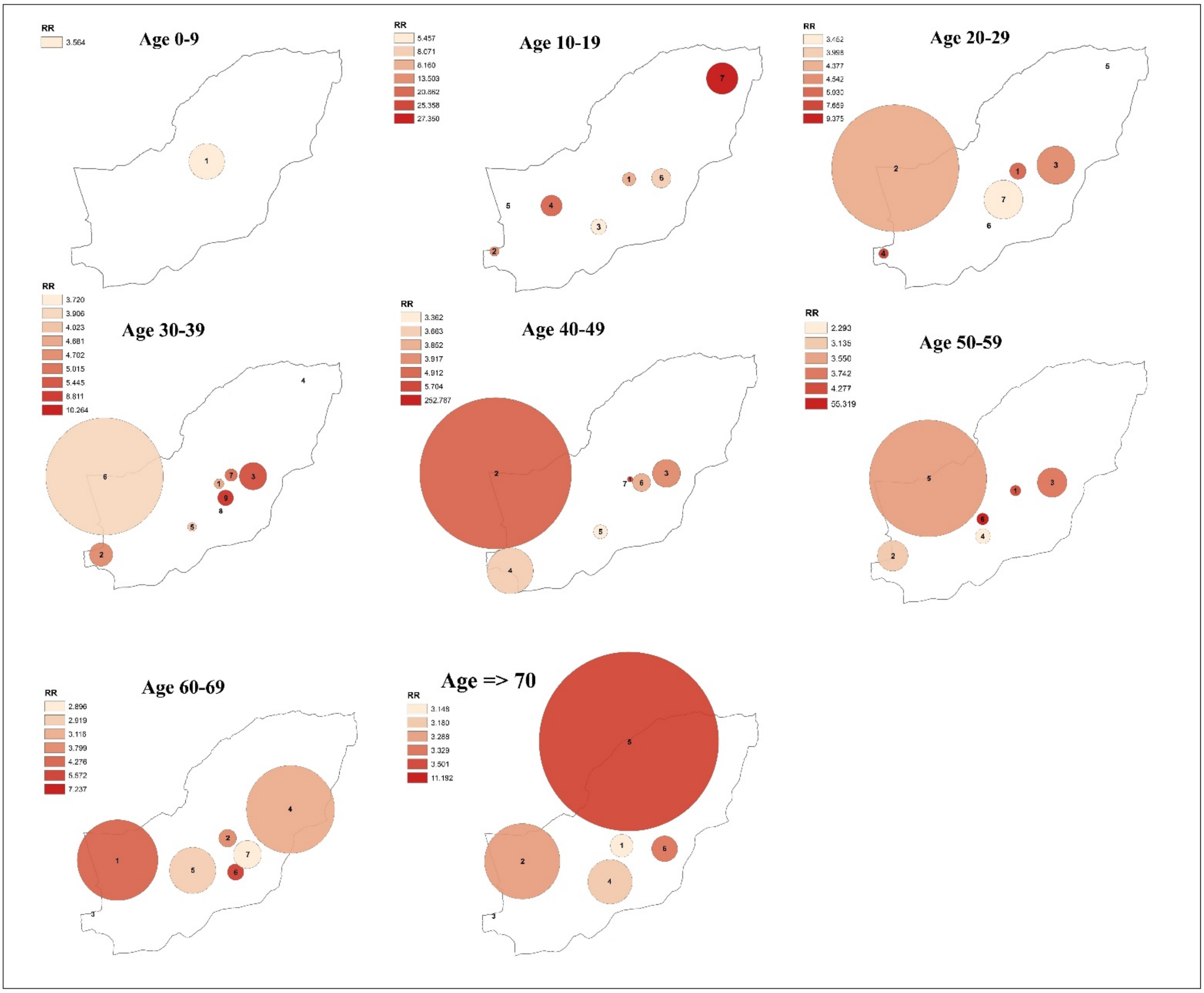

Figure 5. Spatiotemporal clusters of COVID-19 cases by age groups along with their relative risk across the villages/cities of Golestan province between 1 February 2020 and 28 February 2021.

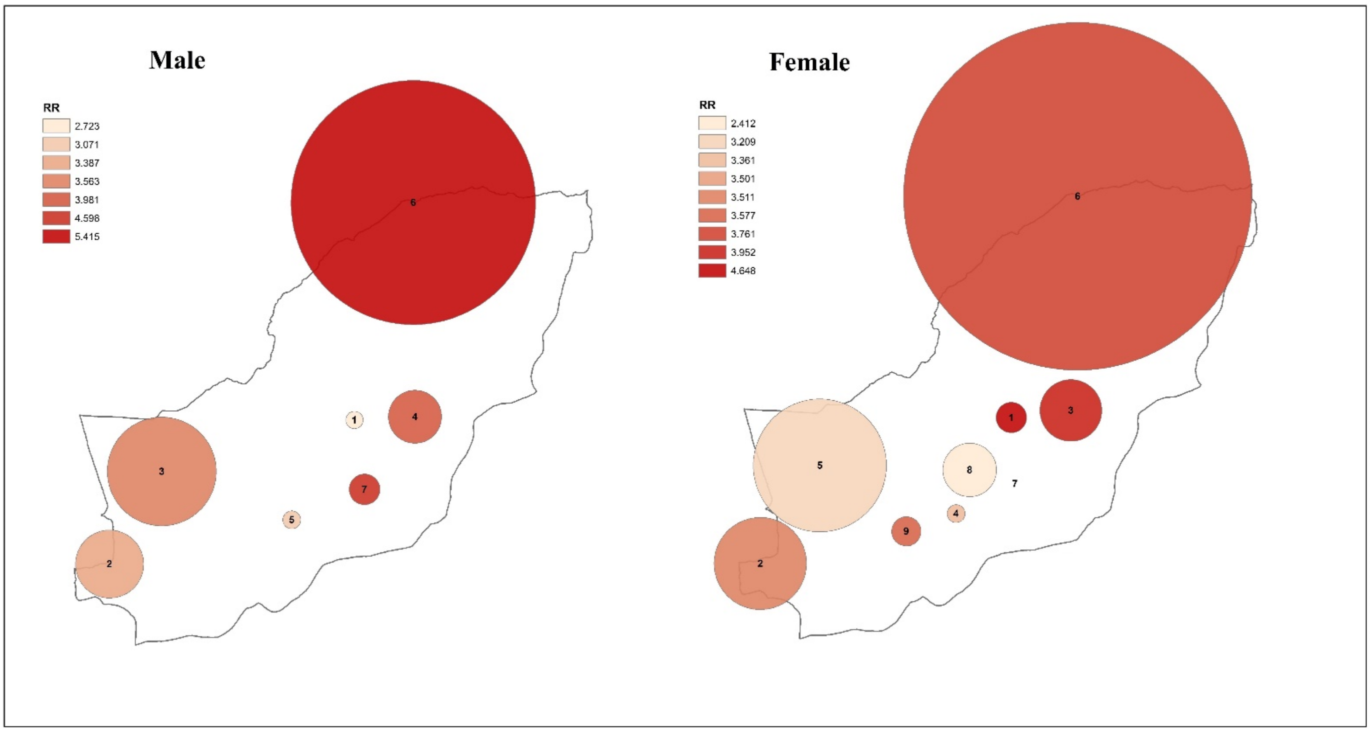

Figure 6. Spatiotemporal clusters of COVID-19 cases by gender along with their relative risk across the villages/cities of Golestan province between 1 February 2020 and 28 February 2021.

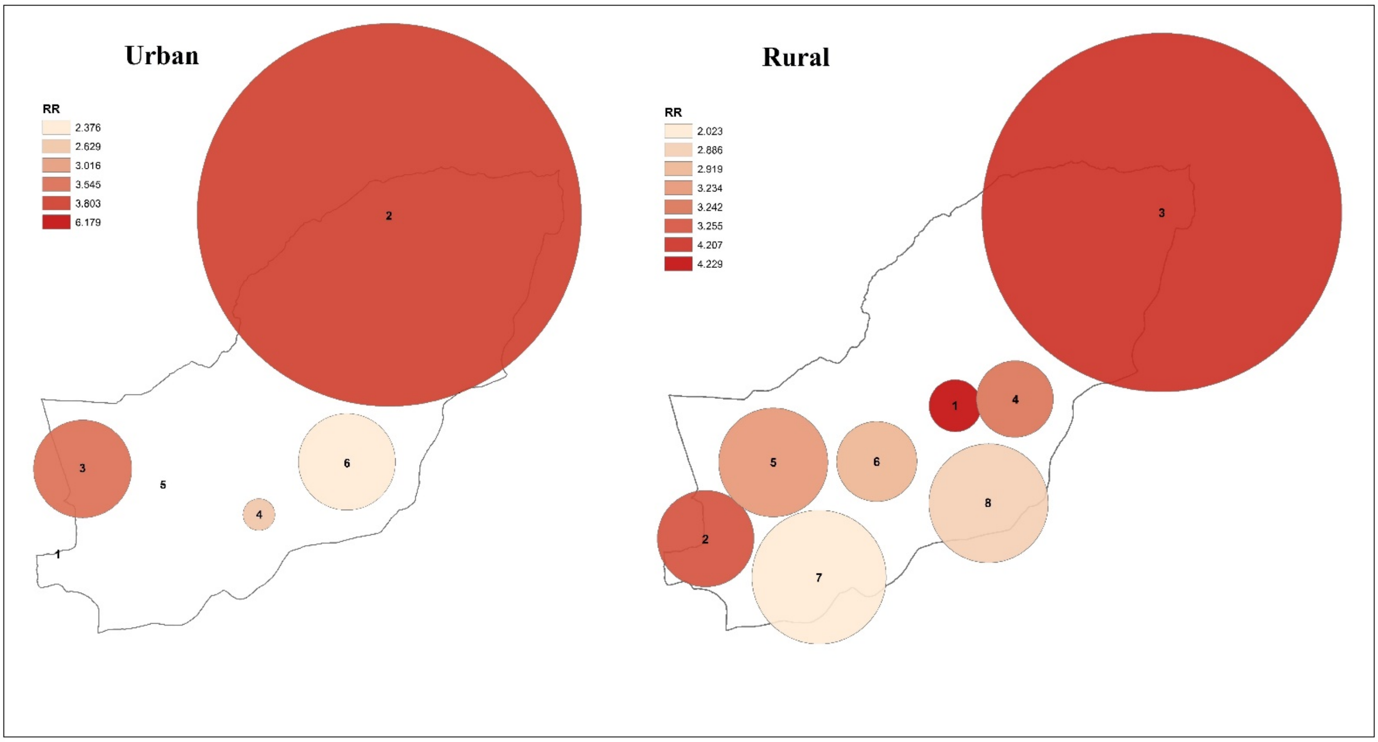

Figure 7. Spatiotemporal clusters of COVID-19 cases based on urban/rural housing along with their relative risk across the villages/cities of Golestan province between 1 February 2020 and 28 February 2021.

4. Discussion

In this retrospective study, temporal and spatial trends of COVID-19 along with spatiotemporal patterns of COVID-19 cases according to the epidemiological characteristics were explored using the space-time scan statistic and spatial analysis in the area of interest from 1 February 2020 to 28 February 2021.

4.1. Main Findings

In terms of temporal trend, despite the public awareness of COVID-19 transmission and considering strict measures against the infection (e.g., quarantining, physical distancing, and using face masks), as the epidemic progressed, the epidemic peaks occurred at a higher number of daily new cases than previous waves in this province (Figure 2), which can be for some reasons. First, insufficient knowledge about the disease by the health officials of the province at the start of the pandemic may lead to a failure in registering the actual number of new cases, in turn, resulting in a smaller number of reported cases than the actual cases. Second, the lack of attention by health authorities to residents of rural areas with limited access to health facilities can explain this unexpected increase. Besides, since proper arrangements had not yet been undertaken to test the suspected cases at the beginning of the epidemic, many people with COVID-19 symptoms were not reported as confirmed cases. However, as testing capacity was increased across the province in early June 2020 (Figure 2), more people with the symptoms referred to the testing sites, causing an increase in the number of daily new cases. In other words, the high positive correlation (0.88%) between the weekly new cases and the weekly testing can explain the increase in COVID-19 in the second wave and subsequent waves. On the other hand, regarding this considerable increase, it seems that control strategies such as mask-wearing, physical distancing, quarantining, and COVID-19 testing have not been sufficient and effective to slow down the transmission in this province during the first year of the pandemic.

The analysis of the epidemiological characteristics in the study area demonstrated that most of the confirmed cases were reported in young adults, supported by an earlier study [18]. It should be noted that the asymptomatic individuals were usually more observed in younger people [37]. Therefore, it is essential to pay close attention to the quarantine of these groups during the pandemic. Most of the reported cases were residents of urban settings, which parallels the previous studies [13,38]. As these areas have higher population density, a more complex transportation system, and more economical and urban facilities than rural areas, a large number of the province's residents visit these areas daily, which in turn increases interactions and social gatherings, intensifying the risk of COVID-19 dissemination in these areas. During the period studied, the case fatality rate (CFR) of COVID-19 in Golestan province was about 2.5 times the average CFR in Iran [20] (9.06% vs. 3.68%). It could be associated with the lack of suitable access to medical facilities for the residents of this province, a low level of adherence of the residents to control measures, and insufficient implementation of preventive policies in this province compared to other provinces of Iran. Based on the census data [39], Golestan province is the fourth province in terms of income inequality (Gini index = 0.3695) among the 31 provinces of Iran. Moreover, this province has a lower average life expectancy than the average life expectancy in Iran, and in this respect, it is the 23rd province. Therefore, the mentioned points could also explain the high CFR in this province. Therefore, policymakers should pay special attention to the residents of this province. In line with prior studies [40,41], diabetes, hypertension, and cardiovascular disease were the most common underlying diseases among COVID-19 patients.

From a spatial perspective, the hot spot analysis revealed that as new waves of the pandemic emerged, residents of the province experienced different outbreaks during the study period. The high prevalence areas were also primarily aggregated in the west, east, and southeast sectors of Golestan. Of 137 hot spots (high-risk villages/cities) identified in the study area, 55 of them are located in Minodasht County, and 28 of them belong to Bandar-e Gaz County. In addition, the directional distribution analysis demonstrated the route of COVID-19 progression throughout the study area, as shown in Figure 3. As of the onset of the epidemic, the virus initially appeared in the western and southwestern regions of the province and gradually propagated to the central, eastern, and southeastern regions. Notably, the heterogeneous spatiotemporal distribution of COVID-19 across the study area suggests that all areas of the province have not responded evenly to the pandemic. Based on Figure 3, the western and southwestern areas of the province, which were the center of COVID-19 transmission until three months after the onset of the epidemic, have become low-risk areas from early May 2020 to the end of November 2020. It may be due to the fact that the health authorities of these regions have taken effective control measures to curb the pandemic. The high adherence of the residents of these areas to the restrictions and quarantine measures can also explain a significant drop in COVID-19 transmission in these regions.

In terms of spatiotemporal patterns, the primary clusters (clusters 1, 2, and 3) of overall COVID-19 cases were mainly concentrated in the east-central and southwest regions of the province, which is spatially consistent with the results of the hot spot analysis (Figures 3 and 4). By the end of May, no significant clusters were observed across the study area, while more dangerous clusters appeared by the beginning of June, confirming the temporal evolution of COVID-19 cases (Table S2 and Figure 2). Among the 12 significant clusters for all COVID-19 cases, clusters 1, 8, and 11 belonged to the second wave of the epidemic, with the highest RR compared to other clusters. These clusters appeared in the east-central areas of the province. The spatial and temporal proximity of these clusters can cause the residents of these areas to have more communication activities with each other, which leads to an increase in the risk of disease in these clusters. These clusters may indicate the existence of health inequalities in these areas. Therefore, health authorities should pay more attention to the residents of these clusters. To our surprise, although most of Golestan's population was mainly distributed in the age group of 0 to 9 years [28], only one significant cluster was detected for this group (Figure 5). This could be due to the lower number of reported cases in this age group (426 cases) compared to other age groups (see S1, Supplementary Materials). On the contrary, the highest number of significant clusters was observed for the age group of 30 to 39 years, which could be due to the higher number of patients in this age group (4624 cases) than in other age groups (see S1, Supplementary Materials). Except for the age group of 60–69, all the most likely clusters for different age groups had almost similar spatial and temporal trends to the most likely cluster identified for all confirmed cases (Figures 4 and 5 and Table S2). Therefore, designing control measures tailored to different age groups in society can be a beneficial guideline to better manage this pandemic. Based on the spatiotemporal clusters by gender, only one significant cluster of the female class has emerged from the onset of the epidemic to the end of the second wave of the epidemic, whereas males have recorded three clusters of the disease in this time frame (Table S2 and Figure 2). It indicates that men were more exposed to the virus than women at the beginning of the pandemic. Since the employment rate of men is higher than that of women in the study area [39], it is expected that men will be more exposed to the virus than women in the communities at the beginning of the epidemic. Unlike the significant clusters of "Hospital discharge" and "Recovered at home", the significant clusters of "Death" mostly happened in the first wave of the epidemic (Table S2 and Figure 2). This could be attributed to the insufficient knowledge of health authorities about the treatment and ways to prevent the virus at the onset of the epidemic. Space-time clusters of comorbidities demonstrate a heterogeneous distribution of underlying diseases across the province, which could result from improper allocation of health facilities to the residents of this province. Yet, there is no clear reason for the observed pattern, and additional work could address this issue. Generally, the identified spatiotemporal clusters describe a story of the space-time COVID-19 propagation throughout the province.

4.2. Strengths

Previous studies recommend that identifying the distribution of COVID-19 cases with regard to epidemiological features provides insights for health policymakers to identify high-risk populations and make a more equitable allocation of medical resources during the outbreak [12,13,24]. To contribute to the literature, this is the first epidemiological study that systematically highlights the spatiotemporal variations of COVID-19 based on epidemiological features in a detailed geographical unit in a region of Iran in the first year of the pandemic. This study not only provides meaningful findings on the time trend of the disease and location of disease aggregation but also identifies more vulnerable groups.

4.3. Limitations

Regardless of the strengths of this research, there are notable limitations that may alter the actual magnitude of the disease propagation. First, the high number of asymptomatic cases in communities increases the number of unreported cases in this study. Secondly, the disease surveillance system in Golestan province is different by county, subjecting the disease data to error. Another significant drawback is related to the spatial window shape in the satscan software. The detected clusters in the Poisson model are circular, which questions the heterogeneous changes in the COVID-19 propagation in the study area. Besides, COVID-19 spread is related to various determinants such as environmental factors, socioeconomic conditions, health capacities, and efficiency of control measures. Exploring them provides a more realistic view of the disease transmission and more targeted interventions in the study area. Although this analysis is beyond the scope of this work, the authors will evaluate the effects of the contributing variables on the disease outbreak across the study area.

5. Conclusions

This explanatory study provides an insight to inform health planners about the issues "When?", "Where?", and "Who?", to explore health inequalities, and to enhance the efficiency of control interventions. Based on the results, it can be concluded that the detected space-time clusters according to epidemiological characteristics were varied throughout Golestan, which can be attributed to different socio-environmental contexts and control interventions implemented across the province. However, additional studies are required to fully understand the reasons behind the observed patterns. In terms of policy implications, this study provides an opportunity for health policymakers to reveal high-risk locations that may have deficient health resource allocation. The results can also be applied to improve early warning systems at the early stages of the pandemic. Another key takeaway of this research is identifying more vulnerable groups, which can be used to optimize the allocation of medical resources.

Supplementary Materials: The following supporting information can be downloaded at: https://www.mdpi.com/article/10.3390/su141912189/s1, S1: The COVID-19 dataset. Table S2: The main characteristics of statistically significant space-time clusters of COVID-19 cases with regard to age, gender, urban/rural housing, patient outcome, and comorbidities across Golestan province from 1 February 2020 to 28 February 2021. Figure S3: Spatiotemporal clusters of COVID-19 cases with regard to patient outcome along with their relative risk across the villages/cities of Golestan province between 1 February 2020 and 28 February 2021. Figure S4: Spatiotemporal clusters of COVID-19 cases with regard to comorbidities along with their relative risk across the villages/cities of Golestan province between 1 February 2020 and 28 February 2021.

Author Contributions: Conceptualization of the study was made by all authors. Data curation, formal analysis, and methodology were performed by M.T. Investigation was carried out by all authors. Project administration was performed by M.T. and A.A.A. Resources were obtained by M.T. and E.B. and software by M.T. Supervision of the study was carried out by A.A.A. Validation of the study was performed by all authors. Funding acquisition was conducted by J.H. M.T. wrote the

original draft of the manuscript, and all authors reviewed and approved the final manuscript. All authors have read and agreed to the published version of the manuscript.

Funding: This publication has been supported by the RUDN University Scientific Projects Grant System, project No 202235-2-000.

Institutional Review Board Statement: Since private information of human records was not used for our study, it was not collected. Thus, preparing ethical approval was not necessary.

Informed Consent Statement: Not applicable.

Data Availability Statement: The data underlying this article are included in Supplementary Materials.

Acknowledgments: The authors gratefully acknowledge the staff of the Center for Disease Control and Prevention (CDC) of Golestan province for their cooperation in sharing the COVID-19 dataset.

Conflicts of Interest: The authors declare no conflict of interest.

References

1. World Health Organization. Novel Coronavirus (2019-nCoV) Situation Reports. 2020. Available online: https://www.who.int/emergencies/diseases/novel-coronavirus-2019/situation-reports (accessed on 4 April 2020).
2. World Health Organization. Laboratory Testing Strategy Recommendations for COVID-19, 2020. 2020. Available online: https://apps.who.int/iris/bitstream/handle/10665/331509/WHO-COVID-19-lab_testing-2020.1-eng.pdf (accessed on 13 April 2020).
3. Tabasi, M.; Alesheikh, A.A. Spatiotemporal variability of Zoonotic Cutaneous Leishmaniasis based on sociodemographic heterogeneity. The case of Northeastern Iran, 2011–2016. *Jpn. J. Infect. Dis.* **2021**, *74*, 7–16. [CrossRef] [PubMed]
4. Babaie, E.; Alesheikh, A.A.; Tabasi, M. Spatial prediction of human brucellosis (HB) using a GIS-based adaptive neuro-fuzzy inference system (ANFIS). *Acta Trop.* **2021**, *220*, 105951. [CrossRef] [PubMed]
5. Mollalo, A.; Vahedi, B.; Rivera, K.M. GIS-based spatial modeling of COVID-19 incidence rate in the continental United States. *Sci. Total Environ.* **2020**, *728*, 138884. [CrossRef] [PubMed]
6. Babaie, E.; Alesheikh, A.A.; Tabasi, M. Spatial modeling of zoonotic cutaneous leishmaniasis with regard to potential environmental factors using ANFIS and PCA-ANFIS methods. *Acta Trop.* **2022**, *228*, 106296. [CrossRef] [PubMed]
7. Tabasi, M.; Alesheikh, A.A.; Sofizadeh, A.; Saeidian, B.; Pradhan, B.; AlAmri, A. A spatio-temporal agent-based approach for modeling the spread of zoonotic cutaneous leishmaniasis in northeast Iran. *Parasites Vectors* **2020**, *13*, 572. [CrossRef] [PubMed]
8. Adekunle, I.A.; Onanuga, A.T.; Akinola, O.O.; Ogunbanjo, O.W. Modelling spatial variations of coronavirus disease (COVID-19) in Africa. *Sci. Total Environ.* **2020**, *729*, 138998. [CrossRef] [PubMed]
9. Melin, P.; Monica, J.C.; Sanchez, D.; Castillo, O. Analysis of spatial spread relationships of coronavirus (COVID-19) pandemic in the world using self organizing maps. *Chaos Solitons Fractals* **2020**, *138*, 109917. [CrossRef]
10. Ceylan, Z. Estimation of COVID-19 prevalence in Italy, Spain, and France. *Sci. Total. Environ.* **2020**, *729*, 138817. [CrossRef]
11. Hernandez-Matamoros, A.; Fujita, H.; Hayashi, T.; Perez-Meana, H. Forecasting of COVID19 per regions using ARIMA models and polynomial functions. *Appl. Soft Comput.* **2020**, *96*, 106610. [CrossRef] [PubMed]
12. Desjardins, M.R.; Hohl, A.; Delmelle, E.M. Rapid surveillance of COVID-19 in the United States using a prospective space-time scan statistic: Detecting and evaluating emerging clusters. *Appl. Geogr.* **2020**, *118*, 102202. [CrossRef] [PubMed]
13. Andersen, L.M.; Harden, S.R.; Sugg, M.M.; Runkle, J.D.; Lundquist, T.E. Analyzing the spatial determinants of local COVID-19 transmission in the United States. *Sci. Total Environ.* **2021**, *754*, 142396. [CrossRef] [PubMed]
14. Xu, M.; Cao, C.; Zhang, X.; Lin, H.; Yao, Z.; Zhong, S.; Huang, Z.; Shea Duerler, R. Fine-scale space-time cluster detection of COVID-19 in Mainland China using retrospective analysis. *Int. J. Environ. Res. Public Health* **2021**, *18*, 3583. [CrossRef] [PubMed]
15. Kan, Z.; Kwan, M.-P.; Wong, M.S.; Huang, J.; Liu, D. Identifying the space-time patterns of COVID-19 risk and their associations with different built environment features in Hong Kong. *Sci. Total Environ.* **2021**, *772*, 145379. [CrossRef] [PubMed]
16. da Silva, W.M.; Brito, P.D.S.; de Sousa, G.G.D.S.; Santos, L.F.S.; da Silva, J.C.; de Jesus Costa, A.C.P.; Pascoal, L.M.; Santos, F.S.; Graepp Fontoura, I.; Lobato, J.S.M.; et al. Deaths due to COVID-19 in a state of northeastern Brazil: Spatiotemporal distribution, sociodemographic and clinical and operational characteristics. *Trans. R. Soc. Trop. Med. Hyg.* **2022**, *116*, 163–172. [CrossRef]
17. Yoneoka, D.; Tanoue, Y.; Kawashima, T.; Nomura, S.; Shi, S.; Eguchi, A.; Ejima, K.; Taniguchi, T.; Sakamoto, H.; Kunishima, H.; et al. Large-scale epidemiological monitoring of the COVID-19 epidemic in Tokyo. *Lancet Reg. Health-West. Pac.* **2020**, *3*, 100016. [CrossRef] [PubMed]
18. Islam, A.; Sayeed, M.A.; Rahman, M.K.; Ferdous, J.; Islam, S.; Hassan, M.M. Geospatial dynamics of COVID-19 clusters and hotspots in Bangladesh. *Transbound. Emerg. Dis.* **2021**, *68*, 3643–3657. [CrossRef] [PubMed]
19. Fonseca-Rodríguez, O.; Gustafsson, P.E.; San Sebastián, M.; Connolly, A.M.F. Spatial clustering and contextual factors associated with hospitalisation and deaths due to COVID-19 in Sweden: A geospatial nationwide ecological study. *BMJ Glob. Health* **2021**, *6*, e006247. [CrossRef]
20. Ritchie, H.; Mathieu, E.; Rodés-Guirao, L.; Appel, C.; Giattino, C.; Ortiz-Ospina, E.; Hasell, J.; Macdonald, B.; Beltekian, D.; Roser, M. Coronavirus pandemic (COVID-19). *Our World Data* **2020**. Available online: https://ourworldindata.org/coronavirus (accessed on 10 February 2022).

21. Bergman, J.; Ballin, M.; Nordström, A.; Nordström, P. Risk factors for COVID-19 diagnosis, hospitalization, and subsequent all-cause mortality in Sweden: A nationwide study. *Eur. J. Epidemiol.* **2021**, *36*, 287–298. [CrossRef] [PubMed]
22. Indseth, T.; Grøsland, M.; Arnesen, T.; Skyrud, K.; Kløvstad, H.; Lamprini, V.; Telle, K.; Kjøllesdal, M. COVID-19 among immigrants in Norway, notified infections, related hospitalizations and associated mortality: A register-based study. *Scand. J. Public Health* **2021**, *49*, 48–56. [CrossRef] [PubMed]
23. Andrade, L.A.; Gomes, D.S.; Lima, S.V.M.A.; Duque, A.M.; Melo, M.S.; Góes, M.A.O.; Ribeiro, C.J.N.; Peixoto, M.V.S.; Souza, C.D.F.; Santos, A.D. COVID-19 mortality in an area of northeast Brazil: Epidemiological characteristics and prospective spatiotemporal modelling. *Epidemiol. Infect.* **2020**, *148*, E288. [CrossRef] [PubMed]
24. Masrur, A.; Yu, M.; Luo, W.; Dewan, A. Space-time patterns, change, and propagation of COVID-19 risk relative to the intervention scenarios in Bangladesh. *Int. J. Environ. Res. Public Health* **2020**, *17*, 5911. [CrossRef]
25. Tyrovolas, S.; Giné-Vázquez, I.; Fernández, D.; Morena, M.; Koyanagi, A.; Janko, M.; Haro, J.M.; Lin, Y.; Lee, P.; Pan, W.; et al. Estimating the COVID-19 spread through real-time population mobility patterns: Surveillance in Low-and Middle-income countries. *J. Med. Internet Res.* **2021**, *23*, e22999. [CrossRef] [PubMed]
26. Map Political Divisions in Golestan Province. Statistical Center of Iran, Deputy of Statistics and Information of Golestan Province. Available online: https://amar.golestanmporg.ir/taghsimat-naghshe.html (accessed on 10 February 2022).
27. COVID-19 Cases Data in Golestan Province. 2020–2021. Iranian Ministry of Health, Center for Disease Control and Prevention (CDC) of Golestan Province (Unpublished Data). 2021. Available online: https://goums.ac.ir/index.php?slc_lang=en&sid=200 (accessed on 28 February 2021).
28. Census Data in Golestan Province. Statistical Center of Iran, Deputy of Statistics and Information of Golestan Province. Available online: https://amar.golestanmporg.ir/ftp/amar/sarshomari/maskan_95/taghsimat-jamiat.xlsx (accessed on 10 February 2022).
29. Celentano, D.D.; Mhs, S.; Szklo, M. *Gordis. Epidemiología*; Elsevier: Amsterdam, The Netherlands, 2019; Available online: https://ak.sbmu.ac.ir/uploads/epidemiology_gordis_5_edi.pdf (accessed on 10 February 2022).
30. Getis, A.; Ord, J.K. The analysis of spatial association by use of distance statistics. In *Perspectives on Spatial Data Analysis*; Springer: Berlin/Heidelberg, Germany, 2010; pp. 127–145.
31. Mitchell, A. *The ESRI Guide to GIS Analysis*; Redlands, CA, USA, 2005; Volume 2, Available online: https://www.esri.com/en-us/esri-press/browse/the-esri-guide-to-gis-analysis-volume-2-spatial-measurements-and-statistics-second-edition (accessed on 10 February 2022).
32. Kulldorff, M. SaTScanTM v8. 0: Software for the Spatial and Space-Time Scan Statistics; Information Management Services, Inc. 2009. Available online: https://www.satscan.org/ (accessed on 10 February 2022).
33. Ahmadkhani, M.; Alesheikh, A.A.; Khakifirouz, S.; Salehi-Vaziri, M. Space-time epidemiology of Crimean-Congo hemorrhagic fever (CCHF) in Iran. *Ticks Tick-Borne Dis.* **2018**, *9*, 207–216. [CrossRef] [PubMed]
34. Kulldorff, M. A spatial scan statistic. *Commun. Stat.-Theory Methods* **1997**, *26*, 1481–1496. [CrossRef]
35. Kulldorff, M. Prospective time periodic geographical disease surveillance using a scan statistic. *J. R. Stat. Soc. Ser. A Stat. Soc.* **2001**, *164*, 61–72. [CrossRef]
36. Gao, P.; Guo, D.; Liao, K.; Webb, J.J.; Cutter, S.L. Early detection of terrorism outbreaks using prospective space–time scan statistics. *Prof. Geogr.* **2013**, *65*, 676–691. [CrossRef]
37. He, J.; Guo, Y.; Mao, R.; Zhang, J. Proportion of asymptomatic coronavirus disease 2019: A systematic review and meta-analysis. *J. Med. Virol.* **2021**, *93*, 820–830. [CrossRef] [PubMed]
38. Paul, R.; Arif, A.A.; Adeyemi, O.; Ghosh, S.; Han, D. Progression of COVID-19 from urban to rural areas in the United States: A spatiotemporal analysis of prevalence rates. *J. Rural Health* **2020**, *36*, 591–601. [CrossRef] [PubMed]
39. Census Data in Golestan Province and Iran. Statistical Center of Iran, Deputy of Statistics and Information of Golestan Province. Available online: https://amar.golestanmporg.ir/ftp/amar/gmoredi/nashriyehtatbighi-1397.pdf (accessed on 10 February 2022).
40. Atkins, J.L.; Masoli, J.A.; Delgado, J.; Pilling, L.C.; Kuo, C.L.; Kuchel, G.A.; Melzer, D. Preexisting comorbidities predicting COVID-19 and mortality in the UK biobank community cohort. *J. Gerontol. Ser. A* **2020**, *75*, 2224–2230. [CrossRef] [PubMed]
41. Baradaran, A.; Ebrahimzadeh, M.H.; Baradaran, A.; Kachooei, A.R. Prevalence of comorbidities in COVID-19 patients: A systematic review and meta-analysis. *Arch. Bone Jt. Surg.* **2020**, *8* (Suppl. S1), 247.